Development/Plasticity/Repair

Lack of Hypoxia-Inducible Factor-1α Impairs Midbrain Neural Precursor Cells Involving Vascular Endothelial Growth Factor Signaling

Javorina Milosevic,[1] Martina Maisel,[2] Florian Wegner,[1] Julia Leuchtenberger,[1] Roland H. Wenger,[3] Manfred Gerlach,[4] Alexander Storch,[2] and Johannes Schwarz[1]

[1]Department of Neurology, University of Leipzig, 04103 Leipzig, Germany, [2]Department of Neurology, Technical University of Dresden, 01307 Dresden, Germany, [3]Institute of Physiology, University of Zürich, 8057 Zürich, Switzerland, and [4]Clinical Neurochemistry, Department of Child and Youth Psychiatry and Psychotherapy, University of Würzburg, 97080 Würzburg, Germany

Oxygen tension is critical for proliferation of human and murine midbrain-derived neural precursor cells (mNPCs). Here, we conditionally inactivated the hypoxia-responsive transcription factor hypoxia-inducible factor-1α (HIF-1α) in murine NPCs to determine its role in proliferation, survival, and dopaminergic differentiation *in vitro* as well as survival of murine dopaminergic neurons *in vivo*. HIF-1α conditional knock-out (HIF-1α CKO) mNPCs showed midbrain-specific impairment of survival and proliferation. Dopaminergic differentiation of HIF-1α CKO mNPCs *in vitro* was markedly reduced. Expression of vascular endothelial growth factor (VEGF) mRNA was reduced in HIF-1α CKO mNPCs, whereas erythropoietin signaling was not affected. Treatment of HIF-1α CKO mNPCs with 50 ng/ml VEGF partially recovered proliferation and dopaminergic differentiation *in vitro*. In substantia nigra (SN) of adult HIF-1α CKO mice, protein levels of dopaminergic marker molecules such as tyrosine hydroxylase (TH) and aldehyde dehydrogenase were reduced by 41 and 61%, respectively. The cell survival marker Bcl-2 was reduced by 58% while caspase-3 was activated. Nonbiased stereological cell counts of TH-positive neurons in SN of young adult HIF-1α CKO mice revealed a reduction of 31% compared with cre/wt mice (in which the wild-type *Hif1a* allele is expressed in parallel with the Cre recombinase allele). However, we found no impairment of striatal dopamine concentrations or locomotor behavior. In conclusion, HIF-1α seems to be a transcription factor relevant to the development and survival of substantia nigra dopaminergic neurons involving VEGF signaling.

Key words: **neural precursor cells; hypoxia; HIF-1α; midbrain; dopaminergic development; apoptosis; VEGF**

Introduction

Neural precursor cells (NPCs) offer a great promise for developing new medical treatments for disorders such as Parkinson's disease (PD) (Gage, 2003; Alvarez-Buylla and Lim, 2004). It is necessary to understand the mechanisms governing cell proliferation, dopaminergic differentiation, and senescence of NPCs to facilitate clinical therapies (Sharpless and DePinho, 2004). Reduced oxygen tension is now recognized as a common requirement for successful expansion and dopaminergic differentiation of NPCs (Ivanovic et al., 2000; Morrison et al., 2000; Studer et al., 2000; Storch et al., 2001; Milosevic et al., 2005). Low, physiologic oxygen conditions help maintain the undifferentiated state in mouse NPCs, but the molecular mechanisms underlying oxygen effects on NPCs are essentially unknown (Milosevic et al., 2005).

Many O_2-responsive genes are regulated via hypoxia-inducible factor-1 (HIF-1), a heterodimer consisting of HIF-1α and HIF-1β (also called aryl hydrocarbon receptor nuclear translocatorm, or ARNT) (Semenza, 1999; Wenger, 2002). HIF-1α abundance is regulated by proteasomal degradation, and its activity is regulated by diverse posttranslational modifications. HIF-1α target genes include vascular endothelial growth factor (VEGF), a potent inducer of angiogenesis, and erythropoietin (EPO). Both have pleiotropic effects in the brain, including neurogenesis and neuroprotection (Sakanaka et al., 1998; Junk et al., 2002; Ferriero, 2005; Greenberg and Jin, 2005), as well as substantial regenerative effects on dopaminergic neurons (Studer et al., 2000; Yasuhara et al., 2005).

HIF-1α is essential for the early development of many mammalian organs including brain (Ryan et al., 1998; Tomita et al., 2003). Mice lacking HIF-1α show severe cardiac and vascular malformations, leading to embryonic lethality at approximately embryonic day 10.5 (E10.5) (Iyer et al., 1998). To study the impact of HIF-1α on NPCs and, in particular, dopaminergic differentiation of midbrain-specific NPCs (mNPCs), we conditionally knocked out HIF-1α exon 2 in NPCs using *Nestin* promoter-

Received June 13, 2006; revised Dec. 4, 2006; accepted Dec. 5, 2006.

This work was supported in part by Interdisziplinäres Zentrum für Klinische Forschung Leipzig Grant TP C27 and the Research Program of the Medical Faculty Carl Gustav Carus of the Technical University of Dresden. We thank Ute Roemuss, Annett Brandt, Sylvia Kanzler, Rainer Burger, and Sabine Gehre for stem cell preparation and/or excellent technical assistance. We thank Dr. Randall S. Johnson for providing HIF-1α-floxed mice.

Correspondence should be addressed to Dr. Javorina Milosevic, Department of Neurology, Max-Bürger-Forschungszentrum, Johannisallee 30, 04103 Leipzig, Germany. E-mail: javorina.milosevic@medizin.uni-leipzig.de.

DOI:10.1523/JNEUROSCI.2482-06.2007

 0270-6474/07/270412-10$15.00/0

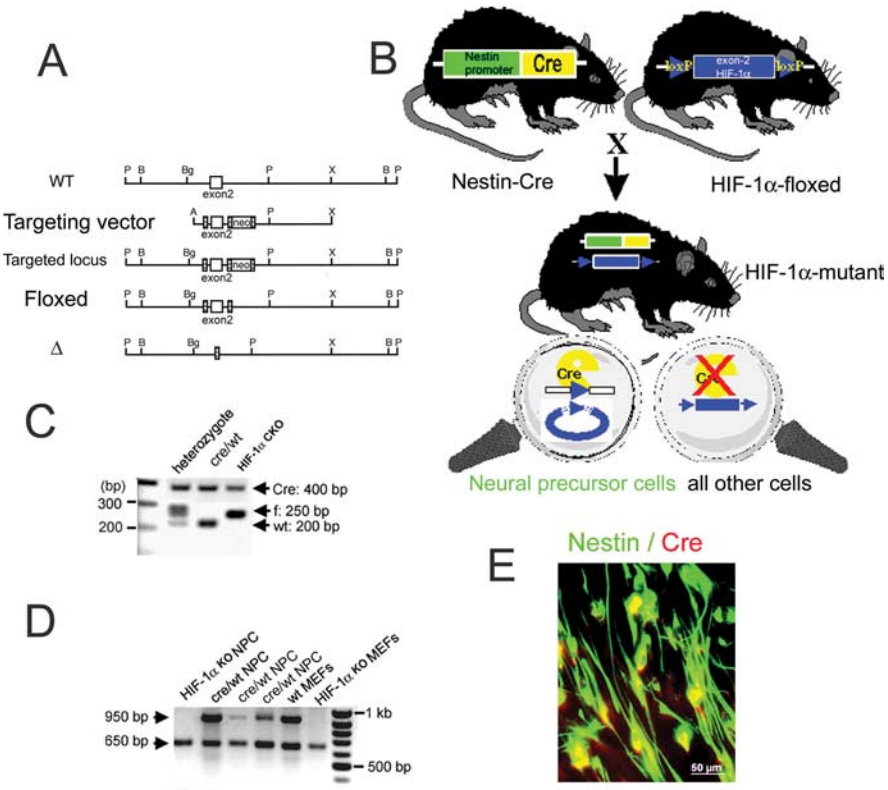

Figure 1. Generation and characterization of neural precursor cells deficient for HIF-1α. ***A***, Exon 2 of the *Hif1a* allele was flanked with *loxP* sites in two steps, resulting in generation of *Hif1a*-floxed mice. Hatched quadrangles represent *loxP* sites. ***B***, *Hif1a*-floxed mice were crossed with *Nestin*–Cre mice to generate HIF-1α mutant mice (*Nestin*–Cre; $Hif1a^{loxP/loxP}$ or HIF-1α CKO mice). ***C***, PCR-based genotyping revealed embryos expressing both floxed *Hif1a* allele (250 bp) and the Cre recombinase (400 bp), identifying double transgenic or HIF-1α conditional mutants (HIF-1α CKO), whereas wild-type *Hif1a* allele (200 bp) and Cre expression identified control (cre/wt) embryos. NPCs dissected from brains of both types of embryos were kept in culture and subjected to additional analysis. NPCs from heterozygous embryos were discarded. ***D***, PCR-based confirmation of Cre-mediated recombination in NPCs. Exon 2 of *Hif1a* was excised by Cre-induced recombination in NPCs, resulting in appearance of a shorter 650 bp band. DNA derived from wt and HIF-1α KO MEFs was used as a positive and a negative control. ***E***, Cre recombinase expression was restricted to NPCs *in vitro* (Nestin-positive), as revealed by double immunofluorescence for Cre and Nestin (yellow color indicates colocalization).

driven expression of *Cre* recombinase (Betz et al., 1996; Rajewsky et al., 1996). Exon 2 encodes the motif necessary for dimerization of HIF-1α and HIF-1β, binding of the HIF-1 dimer to DNA, and its function as a transcription factor (Jiang et al., 1996). Our findings indicate that HIF-1α promotes stem cell survival, growth, and dopaminergic differentiation, as well as survival of adult dopaminergic neurons.

Materials and Methods

Conditional inactivation of HIF-1α in NPCs. A Cre/*loxP* system was used to generate HIF-1α-deficient NPCs (Le and Sauer, 2000; Nagy, 2000). Mice containing *loxP*-flanked *Hif1a* exon 2 ($Hif1a^{loxP/loxP}$ designated as *Hif1a*-floxed mice) were kindly provided by R. S. Johnson (San Diego, CA). The strategy used to obtain *loxP*-flanked *Hif1a* locus instead of the endogenous *Hif1a* locus was described previously (Ryan et al., 2000) (Fig. 1*A*). *Hif1a*-floxed targeted mice were crossed with mice expressing Cre recombinase under the control of the *Nestin* promoter, *Nestin*–Cre transgenic mice (JAXMICE; The Jackson Laboratory, Bar Harbor, ME). *Nestin*–Cre strain of mice was maintained in a C57BL/6 × SJL and *Hif1a*-floxed in a C57BL/6 background. Animals heterozygous for both *Hif1a*-floxed and *Nestin*–Cre alleles were mated to *Hif1a*-floxed homozygous animals to generate *Nestin*–Cre, $Hif1a^{loxP/loxP}$ (HIF-$1\alpha^{\Delta}$) mice. To distinguish HIF-1α conditional knock-out (CKO) embryos/mice, a genomic PCR-based genotyping was applied using the following primers: floxed or wild-type (wt) HIF-1α allele, 5′-GCA GTT AAG AGC ACT AGT TG-3′ and 5′-GGA GCT ATC TCT CTA GAC C-3′, 250 bp product (floxed) or 200 bp product (wild type); Cre recombinase primers, 5′-CCT GGA AAA TGC TTC TGT CCG-3′ and 5′-CAG GGT GTT ATA AGC AAT CCC-3′, 400 bp product (Fig. 1*C*). NPCs were dissected from frontal (fNPCs) or mesencephalic brain regions of HIF-1α null embryos carrying the HIF-1α conditional mutation (HIF-1α CKO fNPCs and HIF-1α CKO mNPCs, respectively) as described below. Removal of HIF-1α exon 2 by Cre-induced recombination in NPCs was confirmed using the following primers: 5′-GCA GTT AAG AGC ACT AGT TG-3′ and 5′-TGT TAA ATA AAA GCT TGG AC-3′, amplifying a 650 bp fragment (Fig. 1*D*).

To exclude possible toxic effects of the Cre recombinase that could influence proliferation of NPCs, in all of our *in vitro* experiments, we compared HIF-1α CKO NPCs with the cells containing the wt *Hif1a* allele expressed in parallel with the *Cre* allele, referred to as cre/wt NPCs (Pfeifer et al., 2001).

Isolation, propagation, and differentiation of NPCs. Mesencephalic and frontal (cortical) NPCs were dissected from mice at E14. Pregnant females were killed according to National Institutes of Health guidelines and the approval of the local animal care committee. Tissue samples were incubated in 0.1 mg/ml papain (Roche, Mannheim, Germany)/DNase solution (100 μg/ml; Roche) for 30 min at 37°C, rinsed in PBS, incubated in antipain (50 μg/ml; Roche) for 30 min at 37°C, and finally homogenized by gentle triturating using a fire-polished Pasteur pipette. The cells were expanded as a monolayer culture by plating onto polyornithine–fibronectin precoated dishes in a density of 20,000 cells/cm^2 (Milosevic et al., 2005). The cells were maintained in serum-free DMEM (high glucose)/F-12 mixture (1:1) medium and supplemented with 20 ng/ml human recombinant epidermal growth factor and 20 ng/ml basic fibroblast growth factor (both from PromoCell, Heidelberg, Germany). NPCs were expanded in 3% oxygen (Storch et al., 2001; Milosevic et al., 2005).

Differentiation of NPCs was induced using defined media without mitogens but with 1% FCS and 5 μM forskolin (Sigma-Aldrich, Munich, Germany). Before electrophysiology, immunocytochemistry, or protein extraction, mNPCs were allowed to differentiate for 1 week. Electrophysiological analysis of mNPCs was also performed after a 20 d differentiation period.

In vitro *VEGF administration.* HIF-1α CKO and cre/wt mNPCs were treated *in vitro* with 50 ng/ml recombinant human VEGF (PAN Biotech, Aidenbach, Germany), applied once for 7 d of proliferation and once during consecutive 7 d differentiation period. Values obtained for treated cultures were normalized to untreated ones.

Clonogenic survival assay. Midbrain-derived or frontal NPCs were seeded in triplicate onto polyornithine–fibronectin precoated six-well plates (1×10^3 cells per well in 3 ml of culture medium). Two weeks after incubation at 37°C in a reduced oxygen (3%) atmosphere, the colonies were fixed in 70% ethanol and stained with 0.5% toluidine blue solution. The number of colonies obtained for cre/wt control NPCs was considered as 100%, and colonies generated by HIF-1α CKO NPCs were normalized to the control cells.

Immunoblotting. Mouse substantia nigra (SN) extracts or NPCs extracts were prepared as described previously (Milosevic et al., 2005). Proteins (50–100 μg) were separated by 12% SDS-PAGE and transferred to nitrocellulose membranes. Antibodies used to probe blots were as

follows: mouse monoclonal anti-proliferating cell nuclear antigen (PCNA) (Santa Cruz Biotechnology, Santa Cruz, CA); mouse monoclonal anti-Bcl-2 (Santa Cruz Biotechnology), mouse monoclonal anti-pro-caspase-3 (BD Transduction Laboratories, San Jose, CA); rabbit polyclonal anti-activated caspase-3 (CM1; BD PharMingen, San Diego, CA); mouse monoclonal anti-VEGF (Abcam, Cambridge, UK); chicken polyclonal anti-aldehyde dehydrogenase (ALDH1A1) (kindly provided by N. E. Sladek, Minneapolis, MN); mouse monoclonal anti-actin (MP Biomedicals, Eschwege, Germany); mouse monoclonal anti-glial fibrillary acidic protein (GFAP) (Chemicon, Hampshire, UK); rabbit polyclonal anti-HIF-1α (Cayman Chemical, Ann Arbor, MI); rabbit polyclonal anti-β-tubulin III (anti-TUJ1; Covance, Richmond, CA); and horseradish peroxidase-conjugated secondary antibodies (Pierce, Rockford, IL).

Immunocytochemistry. NPCs were fixed with 4% paraformaldehyde in PBS for 10 min at room temperature, washed with PBS, and counterstained with the DNA-binding dye 4′-6-diamidino-2-phenylindole (2 μg/ml in PBS) for 15 min at room temperature, twice washed in PBS followed by incubation in blocking buffer (10% FCS and 0.2% Triton X-100 in PBS, pH 7.2) for 30 min at room temperature. After incubation with the primary antibody (1 h at room temperature in blocking buffer), the cells were incubated with fluorescent secondary antibodies, Alexa Fluor 488 conjugate or Alexa Fluor 594 conjugate (Invitrogen, Carlsbad, CA). Coverslips were mounted onto glass slides and examined under a fluorescence microscope (Axiovert 200; Zeiss, Jena, Germany). Acquisition of the cells was performed using the image-analysis software AxioVision 4 (Zeiss, Jena, Germany). The following primary antibodies were used for immunofluorescence: mouse monoclonal anti-nestin (BD Biosciences, San Jose, CA), mouse monoclonal anti-Cre recombinase (Chemicon), and rabbit polyclonal anti-β-tubulin III (anti-TUJ1; Covance).

Confocal microscopy. Activated caspase-3 localization in the SN was investigated by confocal laser scanning microscopy (LSM 510; Zeiss, Oberkochen, Germany) at an excitation wavelength of 594 nm (helium/neon, red Alexa 594 immunofluorescence) and 488 nm (argon, yellow–green Alexa 488 immunofluorescence).

Immunohistochemistry and stereological cell counts. After being fixed by cardiac perfusion (4% paraformaldehyde in phosphate buffer) both HIF-1α KO and cre/wt mice brains were postfixed for 2 h and dehydrated in 15% sucrose and 30% sucrose. Frozen brain samples were cut (40 μm) in a cryostat; 10–20 serial sections from SN levels were collected free floating in ice-cold PBS. Double immunostaining was performed with antisera for tyrosine hydroxylase (TH) (goat polyclonal anti-TH antibody, 1:100; Santa Cruz Biotechnology) and anti-activated caspase-3 (CM1, 1:2000; BD PharMingen), followed by incubation with fluorescent secondary antibodies (1:500, Alexa 488 or Alexa 594; Invitrogen). For stereology, groups of three to four transgenic mice of the same age (4 weeks old) were perfused as described above. TH-positive cells in the SN from HIF-1α CKO and cre/wt mice were selected for nonbiased quantitative stereology. Tissue sections, 40 μm thick (8–12 slices), were chosen for analysis using systematic random sampling. The SN sections were immunostained with a rabbit antibody to TH (rabbit polyclonal; Santa Cruz Biotechnology) at a 1:500 dilution, biotinylated goat anti-rabbit secondary antibody, streptavidin–HRP (Vector Laboratories, Burlingame, CA), and DAB (Sigma-Aldrich). Before dehydration of floating slices, they were processed for Nissl (30 s in 0.5% toluidine blue in PBS) to facilitate counting. The intersection interval, counting frame size, and distance between counting frames were adjusted so that, whenever possible, a reasonable number of TH-stained cells were sampled. The optical fractionator method was used to provide an unbiased estimation of the total number of dopaminergic neurons in the region of interest. Stereologic counting and estimates were done with the aid of Stereoinvestigator version 5.05.1 (MicroBrightField, Magdeburg, Germany) (Orb et al., 2004).

Table 1. Primers for quantitative real-time RT-PCR

Gene (protein)	Primer sequence: forward: reverse	GenBank accession #
Aldoa (aldolase A)	5′-CAA CGG TCA CAG CAC TTC G-3′ 5′-GGC TCG ACC ATA GGA GAA AG-3′	NM_007438
Car9 (carboanhydrase 9)	5′-CGA TTG AGG CTT CCT TCC C-3′ 5′-CTA ACT CTA TCT TTG GTC CCA CTT C-3′	NM_139305
Epo (erythropoietin)	5′-GAA AAT GTC ACG ATG GGT TGT-3′ 5′-TGT TCT TCC ACC TCC ATT CTT T-3′	NM_007942
EpoR (erythropoietin receptor)	5′-CTC ATT CTG GTC CTC ATC TCG-3′ 5′-CAC CAC AGA CAA CCA TCA CG-3′	NM_010149
Gapdh (glycerin-aldehyde-3-phosphatase)	5′-AGG TTG TCT CCT GCG ACT TCA-3′ 5′-GGT GGT CCA GGG TTT CTT ACT C-3′	NM_001001303
Hk1 (hexokinase 1)	5′-GCC ATT GAA ACG GAT AAG GAA-3′ 5′-GGC TGA TCG GAA GGA GAC G-3′	NM_010438
Hmbs (hydroxymethylbilane synthase)	5′-TCG GGG AAA CCT CAA CAC C-3′ 5′-CCT GGC CCA CAG CAT ACA T-3′	NM_013551
Ldha (lactate dehydrogenase A)	5′-GCG GTT CCG TTA CCT GAT G-3′ 5′-GAA CCT CCT TCC ACT GCT CC-3′	NM_010699
Slc2a1 (glucose transporter 1)	5′-GCT TCC TGC TCA TCA ATC GTA A-3′ 5′-CGA CCC TCT TCT TTC ATC TCC T-3′	NM_011400
Slc2a3 (glucose transporter 3)	5′-TCA ACC GCT TTG GCA GAC-3′ 5′-CGA AGG GCA GTG GGA GAC-3′	NM_011401
Vegf (vascular endothelial growth factor)	5′-GCT ACT GCC GTC CGA TTG-3′ 5′-CTG CAG GGC TTC ATC GTT AC-3′	NM_001025257
VEGFR1 = Flk1 (FMS-like tyrosine kinase 1)	5′-GAC ATT ACC TGG ATT CTG CTA CG-3′ 5′-AAG GAT GTC TTC CCC TGT GTA 5-3′	NM_010228
VEGFR2 = Flk1 (fetal liver kinase 1)	5′-GGA CCT GGC AGC ACG AA-3′ 5′-CAC TTC AAA GGG AGT CGG G-3′	NM_010612
VEGFR3 = Flt4 (FMS-like tyrosine kinase 4)	5′-ACG CTG ATG ATA GTC CAC CC-3′ 5′-CGC TGT CTG TCT GGT TAT CC-3′	NM_008029

Electrophysiology. Patch-clamp analysis of mNPCs differentiated *in vitro* for 7 or 20 d was performed at room temperature using an inverted microscope DMIL (Leica, Bensheim, Germany) and an EPC-9 amplifier (HEKA Elektronik, Lambrecht, Germany). Recordings of voltage-gated ion channels were obtained in the whole-cell voltage-clamp mode by stepwise depolarizations with increasing amplitudes from the holding potential of −70 to 50 mV in steps of 10 mV. Series resistance values were continuously measured during all recordings. The external bath solution contained the following (in mM): 142 NaCl, 1 $CaCl_2$, 8 KCl, 6 $MgCl_2$, 10 glucose, and 10 HEPES, pH 7.4 (320 mOsm). Micropipettes were formed from thin-walled borosilicate glass (Science Products, Hofheim, Germany) with a Flaming Brown electrode puller P-97 (Sutter Instruments, Novato, USA) and a Micro Forge (Narishige, Tokyo, Japan). Electrodes had resistances of 2–4 MΩ when filled with the internal solution containing the following (in mM): 153 KCl, 1 $MgCl_2$, 10 HEPES, 5 EGTA, and 2 MgATP, pH 7.3 (305 mOsm). Whole-cell currents were low-pass filtered at 2–5 kHz, digitized at 10 kHz, and analyzed using PulseFit software (HEKA Elektronik) and Prism 4 (GraphPad Software, San Diego, CA). Data were expressed as mean ± SEM. Statistical significance was considered at $p < 0.05$ (Student's *t* test, two-tailed, unpaired).

Determination of dopamine and metabolites. For determination of dopamine, norepinephrine, and their metabolites, striatal tissue was dissected and immediately frozen in liquid nitrogen. Five striata of each genotype were processed. Dopamine, norepinephrine, 3,4-dihydroxyphenylacetic acid (DOPAC), and homovanillic acid were analyzed using standard HPLC techniques essentially as described previously (Gerlach et al., 1996).

Behavioral studies. Sensorimotor performance of HIF-1α CKO compared with cre/wt mice was evaluated using the beam-walk paradigm. Mice were trained to pass a beam for 4 consecutive days. We used a

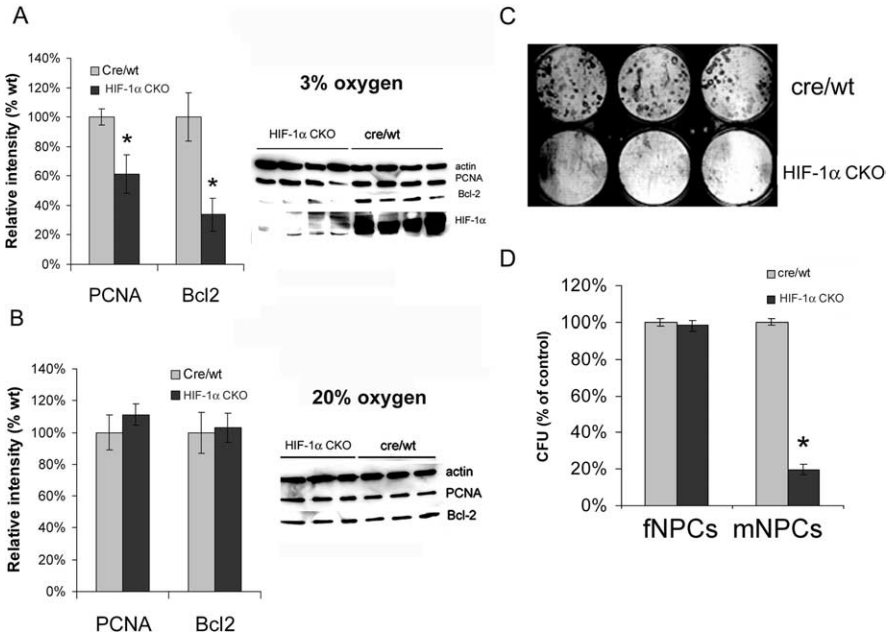

Figure 2. Survival and proliferation of HIF-1α CKO mNPCs are impaired. ***A***, Western blot analysis of HIF-1α wild-type and HIF-1α CKO mNPCs grown in either 3 or 20% oxygen revealed impaired proliferation (PCNA) and survival (Bcl-2) of HIF-1α CKO mNPCs. ***B***, Twenty percent of oxygen caused no changes in expression of PCNA and Bcl-2 in either cre/wt or HIF-1α CKO mNPCs. ***C***, Reduced number of clones formed by HIF-1α CKO versus cre/wt mNPCs in 3% oxygen is shown. ***D***, Numbers of generated colonies [colony-forming units (CFU)], either fNPCs or mNPCs, expressed as a percentage of the colonies formed by cre/wt NPCs. $^*p < 0.05$ compared with cre/wt NPCs.

wooden beam with a length of 1 m, a diameter of 4 mm, and a rough surface to prevent slipping. Mice were motivated via the smell of the food within the target cage. On the fifth day, 10 trials per mouse were analyzed.

Spontaneous locomotion was measured for 30 min using an open-field setup. Transitions from one quadrant to another were scored. All open-field experiments were videotaped and analyzed subsequently by a blinded rater (J.L.).

RNA extraction and quantitative real-time reverse transcription-PCR analysis. Total cellular RNA was extracted from NPCs using RNAeasy total RNA purification kit followed by treatment with RNase-free DNase (Qiagen, Hilden, Germany). Semiquantitative real-time one-step reverse transcription (RT)-PCR was performed using the Stratagene system (MX3000P; Stratagene, Heidelberg, Germany), and amplification was monitored and analyzed by measuring the binding of fluorescent SYBR Green I to double-stranded DNA. One microliter (50 ng) of total RNA was reverse transcribed and subsequently amplified using QuantiTect SYBR Green RT-PCR Master mix (Qiagen) and 0.5 μmol/L of both sense and antisense primers. The sequences for forward and reverse primers used for the target gene (TG) and the reference gene (RG) hydroxymethylbilane synthase are summarized in Table 1. The relative RNA content was determined using the formula of the comparative cycle threshold (Ct): $TG/RG = 2^{Ct(RG) - Ct(TG)}$ (Livak and Schmittgen, 2001). The efficiency of product formation by PCR was estimated from plots of Ct values versus serial dilutions, measured three times with different RNA samples.

Statistical analysis. Normally distributed data were subjected to statistical analyses as indicated (one- or two-way ANOVA) using the SigmaStat software package (Jandel, San Rafael, CA) and Prism 4. Results are expressed as the mean ± SEM. Statistical significance was considered at $p < 0.05$.

Results

Generation and characterization of HIF-1α CKO mNPCs

Hif1a-floxed targeted mice were crossed with mice expressing Cre recombinase under the control of the *Nestin* promoter (*Nestin*–Cre mice) to obtain *Nestin*-Cre; *HIF-1α*$^{loxP/loxP}$ (HIF-1α$^{\Delta}$) mice referred to HIF-1α CKO mice (Fig. 1*A*,*B*). NPCs were dissected from both midbrain and frontal part of each embryonic brain and expanded *in vitro*. After genotyping, only NPCs containing the wt *Hif1a* allele that were cre-positive (cre/wt), as well as NPCs containing the *Hif1α*-floxed allele that were cre-positive (HIF-1α CKO) were kept in culture for additional analysis (Fig. 1*C*,*D*). HIF-1α$^{\Delta/\Delta}$ homozygous mutant myocyte enhancer factors (MEFs) and wt MEFs were used as a negative and positive control for the genotyping (Fig. 1*D*). Immunocytochemical staining confirmed expression of Cre recombinase in Nestin-positive NPCs (Fig. 1*E*).

Wild-type murine NPCs (cre/wt) and NPCs lacking exon 2 of the *Hif1a* gene, designated as HIF-1α CKO dissected from at least four different embryos were expanded in 3% oxygen and checked for expression of HIF-1α protein. In cre/wt NPCs, HIF-1α protein was stabilized in 3% oxygen revealing a 120 kDa band as seen by immunoblotting. This band was not present in HIF-1α CKO cells (Fig. 2*A*). As soon as successful Cre-mediated excision was confirmed in NPCs, these cells were considered as HIF-1α knock-outs.

HIF-1α is important for survival and proliferation of midbrain-derived NPCs

mNPCs generated from at least four different embryos were first expanded for 2 weeks in 3% oxygen and then split for additional expansion for 2 weeks, in either 20 or 3% oxygen. Protein extracts were probed with the proliferation marker PCNA and prosurvival marker Bcl-2. Compared with cre/wt cells, expression of both proteins was significantly reduced in HIF-1α inactive NPCs when they were expanded in 3% oxygen. As shown in Figure 2*A*, PCNA expression was reduced to 61 ± 13% ($n = 4$; $p = 0.035$, one-way ANOVA), whereas Bcl-2 levels were only 34 ± 11% in HIF-1α CKO mNPCs ($n = 4$; $p = 0.015$). When HIF-1α was eliminated by 20% oxygen, PCNA and Bcl-2 expression did not significantly differ in HIF-1α CKO mNPCs compared with cre/wt mNPCs (Fig. 2*B*).

Clonal assays confirmed the necessity of HIF-1α for survival and proliferation of mNPCs. Mesencephalic NPCs derived from HIF-1α CKO embryonic brains in 3% oxygen produced 20 ± 4% colonies normalized to 100% colonies formed by cre/wt NPCs (Fig. 2*C*,*D*).

HIF-1α is not necessary for survival and proliferation of frontal NPCs

To test region-specific effects of HIF-1α deletion in NPCs, we performed the same experimental procedure on frontal NPCs. Proliferation (PCNA protein expression) and survival (Bcl-2 protein expression) assessed by Western blotting did not reveal any significant differences in HIF-1α null compared with cre/wt NPCs in either 3 or 20% oxygen (Fig. 3*A*,*B*). Frontal NPCs derived from HIF-1α CKO embryonic brains in 3% oxygen produced a similar number of colonies compared with cre/wt samples (98 ± 3%) (Fig. 2*D*).

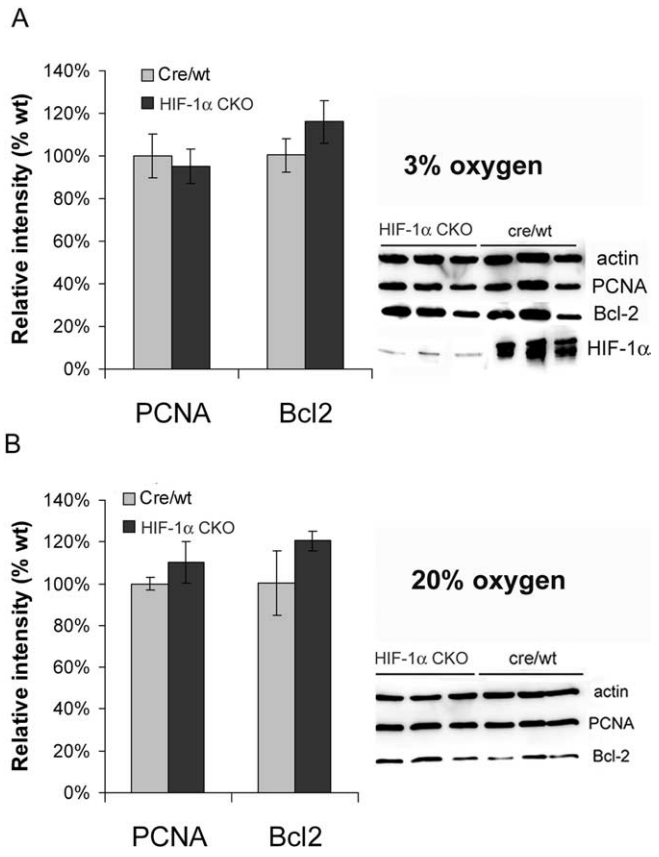

Figure 3. Survival and proliferation of HIF-1α CKO fNPCs. ***A***, ***B***, Western blot analysis of HIF-1α wild-type and HIF-1α CKO fNPCs grown in either 3 or 20% oxygen showed no changes in expression of proliferation marker PCNA and the prosurvival marker Bcl-2.

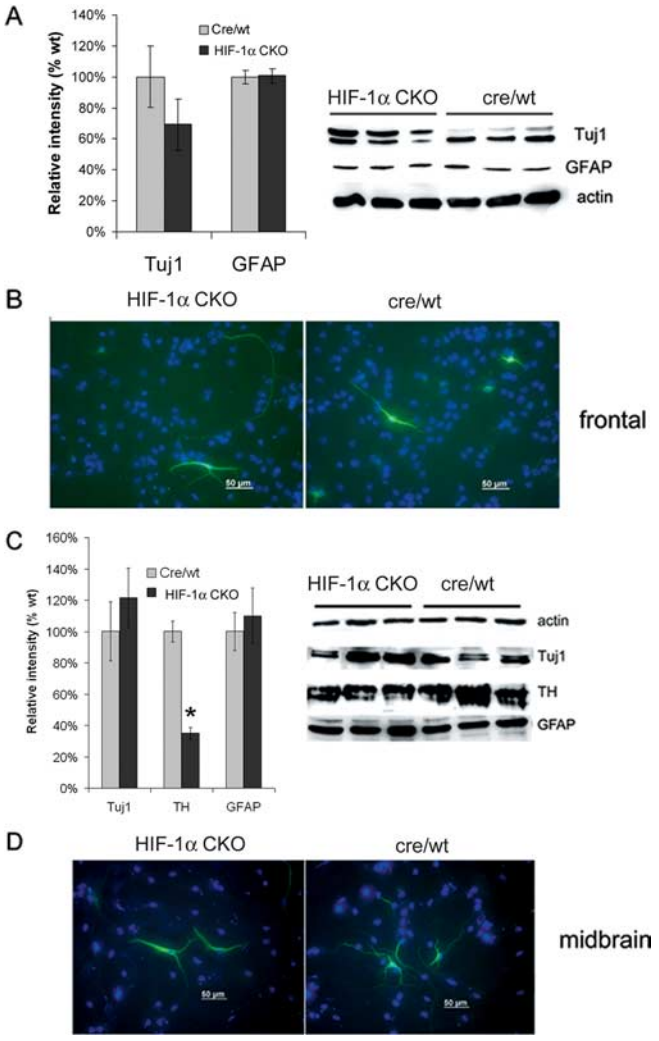

Figure 4. Differentiation potential of frontal (cortical) and mesencephalic NPCs. ***A–D***, Frontal (***A***, ***B***) and mesencephalic (***C***, ***D***) NPCs were first expanded in 3% oxygen for at least eight passages and then were subjected to differentiation for 1 week, which was also in reduced oxygen. Protein extracts were probed with the early neuronal marker β-tubulin III (TUJ1), glial marker (GFAP), marker for dopaminergic neurons (TH), and loading control (β-actin). Data in ***A*** and ***C*** are mean ± SEM values from at least three independent experiments. *$p < 0.05$ when compared with cre/wt NPCs. Immunofluorescence TUJ1 staining of differentiated HIF-1α CKO and cre/wt frontal (***B***) or mesencephalic (***D***) NPCs is shown. Immunostaining of midbrain-derived NPCs has revealed diverse neuronal morphology characterized like reduced axonal branching in CKO versus wt cells.

HIF-1α is important for *in vitro* neuronal and dopaminergic differentiation of midbrain-derived NPCs

Whole-cell extracts for Western blotting were acquired from NPCs after 4 weeks of proliferation and after 1 week of differentiation. Extracts were separated and probed with the neuronal marker (TUJ1), the glial marker (GFAP), or TH, a marker for dopaminergic neurons. As shown in Figure 4*A*, neuronal and glial markers were not significantly changed in fNPCs, whereas differentiated HIF-1α CKO mNPCs exhibited a significant reduction in TH expression, 35 ± 4% of wt ($p < 0.001$). Neuronal differentiation and morphology of NPCs from frontal cortex was not affected by HIF-1α deletion as confirmed by immunocytochemical analysis of frontal NPCs (Fig. 4*B*). In both KO and cre/wt differentiated fNPCs, extensive neuronal processes were observed. Furthermore, protein expression of TUJ1 and GFAP did not vary between two different cell types (Fig. 4*C*). However, TUJ1 staining on cultured mNPCs 1 week after differentiation in 3% oxygen showed an altered morphology in HIF-1α CKO mNPC compared with cre/wt NPCs. Cre/wt neurons were more mature, exhibiting longer neurites (Fig. 4*D*).

Electrophysiological analyses of voltage-gated ion channels showed significantly decreased maximal sodium inward currents of HIF-1α CKO mNPCs (116.9 ± 33.9 pA) 7 d after *in vitro* differentiation compared with cre/wt NPCs (318.2 ± 77.7 pA; $n = 12$ for each genotype; $p = 0.032$, *t* test), whereas no significant reduction was calculated for potassium outward rectifying currents (Fig. 5). After 20 d of mNPC differentiation, values for sodium and potassium currents were increased in both HIF-1α CKO and cre/wt cells without altering the difference between the two genotypes (data not shown). In contrast, there was no significant difference in maximal amplitudes of sodium and potassium currents between HIF-1α CKO and cre/wt frontal NPCs 7 d after *in vitro* differentiation (data not shown).

HIF-1α supports the development and/or survival of dopaminergic neurons

SN was dissected from 4-week-old HIF-1α CKO mice and their cre/wt littermates. At the time of analysis, these animals were macroscopically identical. Tissue extracts were analyzed via immunoblotting. Neuronal β-tubulin III (TUJ1) expression did not significantly differ between genotypes, whereas TH protein was reduced to 59 ± 5% in HIF-1α CKO mice ($n = 5$; $p = 0.008$, *t* test). The expression of ALDH1A1, another early marker of SN dopaminergic neurons, was reduced to 39 ± 19% ($n = 5$; $p = 0.002$). Prosurvival protein Bcl-2 was reduced to 43 ± 12% ($n =$

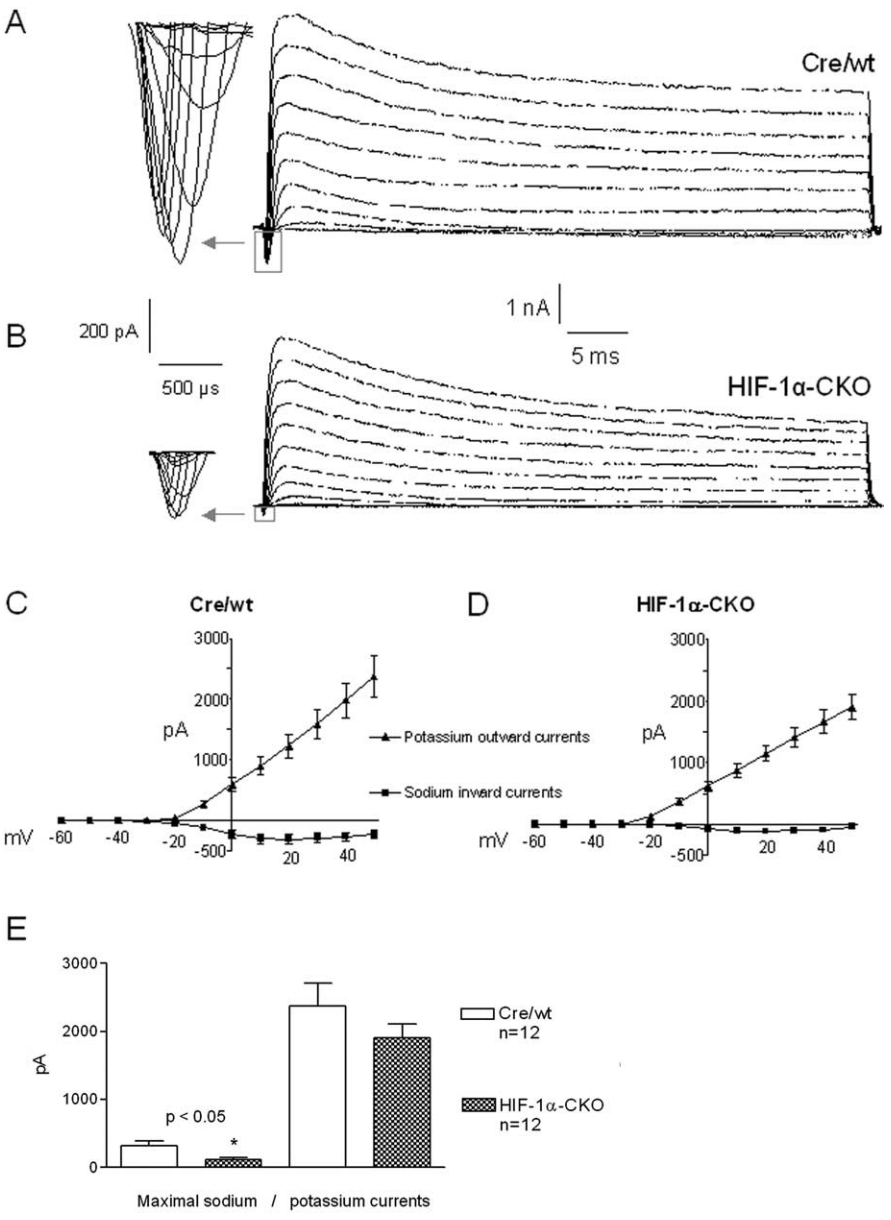

Figure 5. Voltage-gated ion channels of murine mesencephalic NPCs after 7 d *in vitro* differentiation. ***A***, ***B***, Recordings of cre/wt (***A***) and HIF-1α CKO (***B***) cells were obtained in whole-cell voltage-clamp mode by stepwise depolarizations with increasing amplitudes from the holding potential of −70 to 50 mV in steps of 10 mV. Note the inlays showing sodium inward currents that were more pronounced in cre/wt (***A***) than in HIF-1α CKO (***B***) cells. ***C***, ***D***, Current–voltage plots of mNPCs show higher values for mean amplitudes of sodium inward and potassium outward currents in cre/wt (***C***) than in HIF-1α CKO (***D***) cells. Maximal sodium inward currents (***E***) of HIF-1α CKO NPCs were significantly decreased compared with cre/wt cells ($p = 0.032$, *t* test), whereas no significant reduction was calculated for potassium outward rectifying currents; all current values are shown as means ± SEM.

5; $p = 0.03$). Pro-caspase-3 was cleaved in HIF-1α CKO mice SN extracts, resulting in reduced levels of 20 ± 15% ($n = 5$; $p = 0.008$), but activated caspase-3 was increased because it was not detectable in extracts from cre/wt mice. VEGF protein was reduced in SN taken from HIF-1α CKO compared with cre/wt mice (Fig. 6*A*). Double-immunofluorescence labeling of brain slices in combination with confocal laser scanning microscopy indicated that the activated, cleaved form of the caspase-3 was predominantly present in dopaminergic (TH-positive) cells in the SN of HIF-1α CKO mice (Fig. 6*B*). In the SN of cre/wt mice, we could not find any cells positive for both caspase-3 and TH.

Finally, stereological non-biased counts of TH-positive cells in the SN of HIF-1α CKO mice ($n = 4$) showed a robust and significant reduction compared with cre/wt SN (total number of TH-positive neurons in the SN, 7489 ± 477 vs 10,817 ± 903, respectively, or 69 ± 6% of cre/wt) (Fig. 6*C*). However, the number of TH-positive cells in another brain region, ventral tegmental area (VTA), remained unaffected ($n = 4$) (Fig. 6*C*). Nissl staining of both cre/wt and HIF-1α CKO brain slices revealed no difference in the SN (50,096 ± 246 vs 48,913 ± 2006, respectively; $n = 3$), dentate gyrus (375,897 ± 61,210 vs 364,628 ± 30,580), and medial habenula (84,560 ± 6141 vs 79,318 ± 5740). In addition, biochemical measurements of dopamine, norepinephrine, and their metabolites (DOPAC and HVA) did not reveal any significant differences between genotypes (data not shown). These findings are well in line with other mouse models of Parkinson's disease, in which moderate losses of dopaminergic neurons within SN are readily compensated (Orb et al., 2004).

An evaluation of potential sensorimotor deficits using analysis of beam walking and spontaneous locomotion failed to show any difference between genotypes (data not shown). Open-field behavior of HIF-1α CKO and cre/wt mice was quantified for 30 min. Statistical analysis by two-tailed *t* test revealed no statistical differences between HIF-1α CKO and cre/wt mice ($n = 7$ of both genotypes).

Expression analysis of HIF-1α-regulated genes revealed VEGF and VEGF receptors as major downstream genes of HIF-1α in mNPCs

The expression of VEGF and VEGF receptor (VEGFR) subtypes as HIF-1α regulated genes was explored and quantified in expanded mNPCs and fNPCs by real-time RT-PCR. VEGF expression was reduced in HIF-1α CKO mNPCs compared with both cre/wt mNPCs and fNPCs ($n = 7$; $p = 0.036$) (Table 2, Fig. 7*A*) but showed no change between both fNPC subtypes. Expression levels of VEGFR-1 (Flt-1) were significantly higher in mNPCs compared with fNPCs independent of HIF-1α expression (Table 2). VEGFR-2 (Flk-1) expression was 2.7- to 3.8-fold increased in HIF-1α CKO compared with cre/wt NPCs in both mesencephalic and frontal NPCs and 31- to 44-fold higher in mNPCs compared with fNPCs independent of HIF-1α expression ($n = 4$; $p = 0.018$) (Table 2, Fig. 7*A*). VEGFR-3 (Flt-4) expression did not differ between HIF-1α CKO and cre/wt mNPCs. We did not detect differences in mRNA levels of the EPO receptor (EPOR) in HIF-1α CKO and cre/wt mNPCs and fNPCs (data not shown). Additionally, there were no detectable mRNA levels of EPO in all four cell types. Significantly lower expression of neuronal glucose transporter 3 (*Slc2a3*) in both fNPC subtypes and in HIF-1α

CKO mNPCs compared with cre/wt mNPCs were seen (Table 2). In contrast, we did not detect significant differences in mRNA levels of various other non-neuronal HIF-1α-regulated genes with respect to the four NPC subtypes (Table 2).

VEGF stimulates proliferation and dopaminergic differentiation of HIF-1α CKO mNPCs *in vitro*

Because VEGF seemed to be reduced in HIF-1α CKO mNPCs and potentially mediate the effects of HIF-1α in these cells, we tried to rescue HIF-1α CKO mNPCs by supplementing culture media with VEGF. Proliferation, analyzed by PCNA expression, was significantly increased in HIF-1α CKO mNPCs after application of VEGF (50 ng/ml) (47 ± 5% in untreated vs 75 ± 4% in VEGF-treated cells; $p < 0.05$, two-way ANOVA). In addition, TH protein was elevated from 26 ± 5% of control in untreated HIF-1α CKO mNPCs to 68 ± 6% after VEGF treatment ($n = 4$; $p < 0.05$) (Fig. 7*B*,*C*). Proliferation of cre/wt cells did not significantly change after VEGF treatment. The prosurvival protein Bcl-2 and the neuronal marker TUJ1 were not altered by VEGF treatment in either cell type (Fig. 7*B*,*C*). Thus, only partial recovery of HIF-1α CKO mNPCs proliferation and differentiation was induced by VEGF *in vitro* administration.

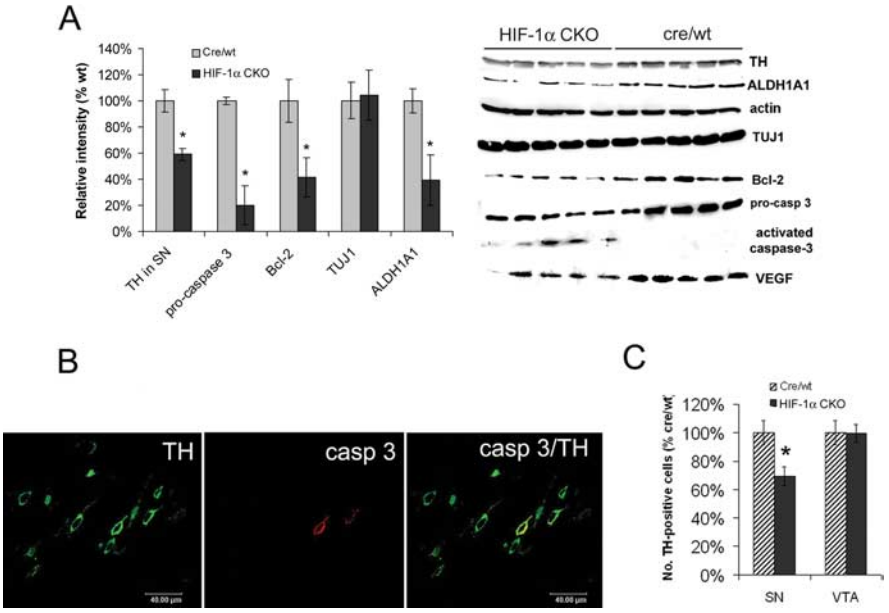

Figure 6. Degeneration of the SN of HIF-1α CKO mice. ***A***, Immunoblots demonstrating TH and ALDH1A1 protein expression, neuronal β-tubulin III (TUJ1) expression, apoptotic effectors such as Bcl-2, pro-caspase-3, and activated caspase-3, and HIF-1α downstream target genes such as VEGF, all parallel assessed in the SN of HIF-1α CKO and cre/wt mice. ***B***, SN of HIF-1α CKO mice viewed by confocal microscopy showing colocalization of activated caspase-3 (CM1; red) in TH-immunoreactive cells (green). ***C***, Stereological investigation revealing the number of dopaminergic (TH-positive) neurons in the SN and the ventral tegmental area of HIF-1α CKO in relation to cre/wt mice is presented. Scale bar, 40 μm. Data are expressed as mean ± SEM values from five independent experiments. *$p < 0.05$ when compared with cre/wt NPCs.

Discussion

Here we demonstrate for the first time that HIF-1α is important for proliferation, survival, and differentiation of murine tissue-specific midbrain-derived NPCs. Thus, HIF-1α may be an essential mediator with respect to the beneficial effects of lowered oxygen tension on NPCs (Studer et al., 2000; Storch et al., 2001; Milosevic et al., 2005). Adult HIF-1α-deficient mice also showed deficits of SN dopaminergic neurons, indicating that HIF-1α is not only important for proliferation and differentiation of mNPCs *in vitro* but may also mediate regeneration or survival *in vivo*.

Gas phase oxygen concentrations of 1–5% correspond to the physiological environment in embryonic tissue and adult brain (Silver and Erecinska, 1998). These "physiological" concentrations seem to be required for stem cell maintenance (Gustafsson et al., 2005; Covello et al., 2006). Recently, we demonstrated that "room air" damages murine midbrain-derived NPCs, initiating a variety of cellular events (Milosevic et al., 2005). However, it was not clear whether 3% oxygen affects NPC proliferation and differentiation via an HIF-1-dependent signaling pathway or via another mechanism.

Table 2. Gene expression profile of HIF-1α-regulated genes in NPCs grown under 3% oxygen condition[a]

Genes (protein)	HIF-1α CKO mNPCs	cre/wt mNPCs	HIF-1α CKO 1NPCs	cre/wt fNPCs	*p* value[b]
Aldoa (aldolase A)	5.66 ± 0.66	6.94 ± 2.02	6.88 ± 1.31	9.45 ± 0.76	0.16
Car9 (carboanhydrase 9)	0.01 ± 0.00	0.02 ± 0.01	0.06 ± 0.02	0.14 ± 0.09	0.10
Epo (erythropoietin)	n.d.	n.d.	n.d.	n.d.	
EpoR (erythropoietin receptor)	0.07 ± 0.01	0.06 ± 0.01	0.06 ± 0.02	0.09 ± 0.02	0.69
Gapdh (glycerin-aldehyde-3-phosphatase)	93.1 ± 24.7	166.2 ± 34.6	173.1 ± 43.0	278.6 ± 21.9	0.24
Hk1 (hexokinase 1)	2.71 ± 0.23	1.96 ± 0.35	1.71 ± 0.24	2.56 ± 0.20	0.23
Ldha (lactat deydrogenase A)	26.0 ± 2.54	74.4 ± 21.3	31.3 ± 2.29	57.6 ± 6.79	0.18
Slc2a1 (glucose transporter 1)	0.65 ± 0.05	1.24 ± 0.61	0.92 ± 0.43	1.92 ± 0.88	0.38
Slc2a3 (glucose transporter 3)	0.16 ± 0.01*	0.38 ± 0.06	0.07 ± 0.02*$^{++}$	0.17 ± 0.04^{++}	0.00015
Vegf (vascular endothelial growth factor)	8.85 ± 2.42*	18.7 ± 8.9	13.7 ± 1.4^{+}	18.4 ± 6.1	0.036
VEGFR1/Flt1 (VEGF receptor 1/FMS-like tyrosine kinase 1)	0.21 ± 0.11	0.19 ± 0.07	0.04 ± 0.03^{+}	0.07 ± 0.02^{+}	0.028
VEGFR2/Flk1 (VEGF receptor 2/fetal liver kinase 1)	0.30 ± 0.06*	0.11 ± 0.06	0.0095 ± 0.001**$^{,++}$	0.0025 ± 0.001^{++}	0.0008
VEGFR3/Flt4 (VEGF receptor 3/FMD-like tyrosine kinase 4)	0.07 ± 0.03	0.11 ± 0.09	0.0029 ± 0.001	0.0039 ± 0.001	0.19

n.d., Not detectable.

[a] mRNA levels of the target gene relative to the housekeeping gene *Hmbs* (mean ± SEM) from three to seven experiments.

[b] *p* values from ANOVA tests for multiple group comparisons (n = 3–7); *post hoc t* test revealed statistical significant differences with *$p < 0.05$ and **$p < 0.01$ when compared with control NPCs (cre/wt mNPCs or cre/wt fNPCs); $^{+}p <$ 0.05 and $^{++}p < 0.01$ when compared with the respective mNPC subtype.

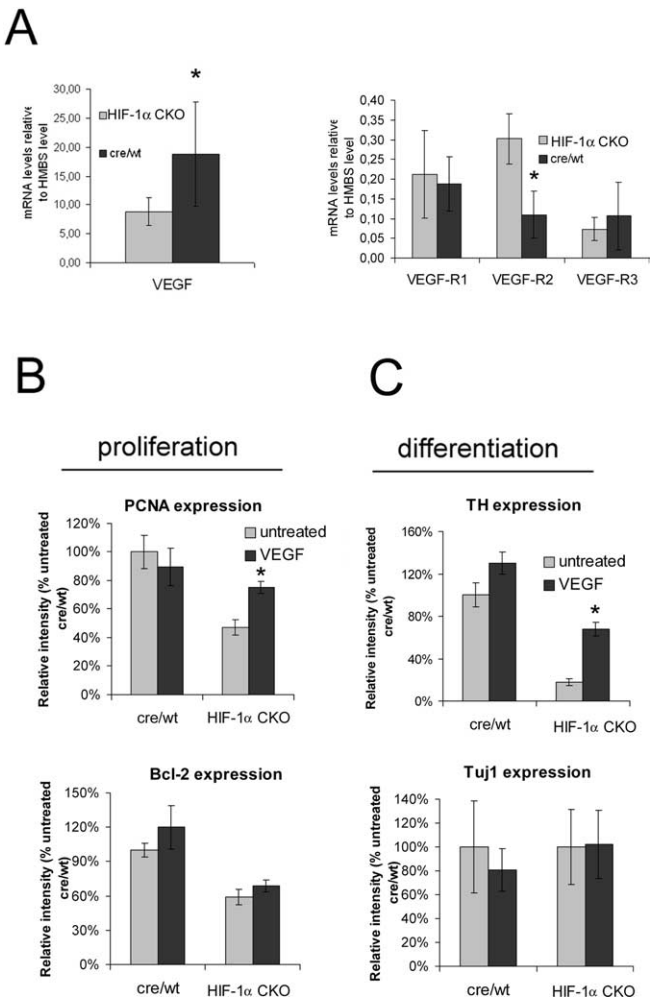

Figure 7. VEGF partially restores proliferation and dopaminergic differentiation of HIF-1α CKO mesencephalic NPCs expanded in 3% oxygen. ***A***, Compared with cre/wt, VEGF mRNA expression is reduced in HIF-1α CKO mNPCs, whereas VEGFR-2 expression is increased in the CKO as observed by semiquantitative RT-PCR analysis. ***B***, ***C***, Proliferation (***B***) (PCNA and Bcl-2 protein expression) and differentiation (***C***) (TH protein expression, TUJ1 expression) markers observed in HIF-1α CKO mNPC untreated and treated with VEGF relative to cre/wt untreated values are shown. VEGF (50 ng/ml) was applied for 7 d of proliferation followed by 7 d of differentiation. Data are mean ± SEM values from at least four independent experiments. $*p < 0.05$ when compared with cre/wt mNPCs.

In an attempt to elucidate the role of HIF-1α in 3% oxygen-stimulated survival, proliferation, and differentiation in murine NPCs, we conditionally targeted HIF-1α in NPCs using a Cre/*loxP*-based system (Ryan et al., 2000). Tomita et al. (2003) created mice with neural-cell-specific HIF-1α deficiency, exhibiting hydrocephalus, neuronal loss, and impairment of spatial memory. In the present paper, we focused on the midbrain dopaminergic system, investigating possible alterations of dopaminergic markers (ALDH1A1, TH, dopamine, and metabolites) and expression of major HIF-1α downstream proteins, such as VEGF and EPO. Deletion of HIF-1α in mNPCs had an impact on neuronal morphology *in vitro* accompanied by a significant reduction of sodium inward currents elicited by depolarizations, suggesting an altered morphological and functional differentiation compared with cre/wt mNPCs. In this regard, cortical NPCs remained unaffected. Midbrain-derived NPCs also showed decreased levels of TH after differentiation. In contrary to the major finding by Tomita et al. (2003), which was apoptosis in the cortical plate resulting in cortical atrophy in HIF-1α null mutant mice, we did not observe any significant changes regarding proliferation, survival, and neuronal differentiation in frontal (cortical) NPCs. In addition, we did not notice any alterations in cortical brain regions in 4-week-old mice, which, according to Tomita et al. (2003), at that age should have been visible. Our HIF-1α CKO mice were macroscopically indistinguishable from cre/wt mice but exhibited morphological alterations in the SN. However, our mice did not show major locomotor deficits or dopamine deficiency within striatal tissue, suggesting that the moderate loss of dopaminergic neurons at that age was well compensated. HIF-1α functional mutants developed by Tomita et al. (2003) were created also using Cre/*loxP* technology but excising exons 13–15 of the HIF-1α gene while we excised exon 2. HIF-1α mutant protein in the report by Tomita et al. (2003) lacked the transactivation domain, whereas our HIF-1α mutant mice lack the DNA binding domain. Thus, the HIF-1α mutant protein was either absent or functionally inert (Jiang et al., 1996; Ema et al., 1999). At this point, it is not clear whether the differences seen between two HIF-1α CKO mice originate as a consequence of a different genetic manipulation, differences in genetic background, or other reasons.

HIF-1α might be protective in some neurological disorders (Soucek et al., 2003). Neuroprotective effects of EPO on dopaminergic neurons suggested a possible positive effect of hypoxia via HIF-1α and subsequent EPOR expression (Demers et al., 2005). In line with recent studies suggesting a pivotal role of HIF-2α in regulating EPO expression (Chavez et al., 2006), we did not find relevant EPO expression in our cell system and no differences of EPOR expression in HIF-1α CKO versus cre/wt mNPCs, suggesting that EPOR signaling is not involved in HIF-1α-dependent survival, proliferation, and differentiation of mNPCs. Conversely, VEGF as another downstream target gene of HIF-1α acts as a direct neurotrophic or even neuroprotective factor (Matsuzaki et al., 2001; Sun et al., 2003). We detected a notable reduction in VEGF mRNA expression in HIF-1α CKO compared with cre/wt mNPCs and a most likely compensatory upregulation of VEGFR-2. SN of HIF-1α CKO mice expressed less VEGF protein compared with cre/wt. We further demonstrated that proliferation and dopaminergic differentiation of HIF-1α CKO mNPCs were partially recovered after *in vitro* administration of VEGF, indicating that other target genes besides VEGF are involved. The lack of HIF-1α coincided with apoptotic cell death in dopamine-producing, TH-positive cells in the SN of adult mice. Procaspase-3 was cleaved in the SN of HIF-1α CKO mice confirmed by *in situ* caspase-3 activation. Expression of the anti-apoptotic protein Bcl-2 in SN of HIF-1α CKO mice was decreased, likely as a consequence of an effector caspase activation (Milosevic et al., 2003). However, HIF-1α CKO mice exhibited absence of gross locomotor and sensorimotor behavioral deficits, which is in line with other mouse models with moderate dopaminergic deficits (Masliah et al., 2000; Orb et al., 2004).

HIF-1α activates the expression of hypoxia-inducible genes that contain a hypoxia response element located in the promoter or enhancer regions. Hypoxia induces TH mRNA expression in rat mesencephalic cultures (Leclere et al., 2004), whereas HIF-1α contributes to induction of TH transcription in PC12 cells (Schnell et al., 2003). Our findings indicate that HIF-1α represents an important factor for *in vitro* neuronal and dopaminergic differentiation, as well. Conditional knock-

out of HIF-1α affected SN neurons in young adult mice. In addition to the decline of TH expression, we observed a reduction in another neuronal marker enriched in SN, ALDH1A1. ALDH1A1 is shown to be expressed in A9 dopaminergic neuronal group, the most vulnerable site in PD (Chung et al., 2005). We showed a prominent reduction in the number of dopaminergic (TH-positive) neurons in the SN of HIF-1α-deficient mice. Many animal models with degeneration of dopaminergic neurons show specificity for dopaminergic neurons in SN compared with VTA (Liss et al., 2005; Maingay et al., 2006). Accordingly, HIF-1α-deficient mice have no deficit in A10 dopaminergic neurons. Moreover, as revealed by Nissl staining, other neuronal types (e.g., GABAergic neurons in gyrus dentatus or SN, catecholaminergic neurons in medial habenula) likely also remained unaffected in HIF-1α CKO, because examined brain regions did not exhibit difference in neuronal cell numbers when compared with cre/wt mice.

Our data represent first evidence for a role of HIF-1α for dopaminergic development and survival. We also identified an important downstream gene: VEGF. However, because VEGF supplementation only partly antagonizes the lack of HIF-1α, future studies need to identify other downstream targets of HIF-1α that mediate this effect and may therefore represent potential drug targets for regeneration or protection of SN dopaminergic neurons, the cell type selectively affected in Parkinson's disease.

References

Alvarez-Buylla A, Lim DA (2004) For the long run: maintaining germinal niches in the adult brain. Neuron 41:683–686.

Betz UA, Vosshenrich CA, Rajewsky K, Muller W (1996) Bypass of lethality with mosaic mice generated by Cre-loxP-mediated recombination. Curr Biol 6:1307–1316.

Chavez JC, Baranova O, Lin J, Pichiule P (2006) The transcriptional activator hypoxia inducible factor 2 (HIF-2/EPAS-1) regulates the oxygen-dependent expression of erythropoietin in cortical astrocytes. J Neurosci 26:9471–9481.

Chung S, Hedlund E, Hwang M, Kim DW, Shin BS, Hwang DY, Jung Kang U, Isacson O, Kim KS (2005) The homeodomain transcription factor Pitx3 facilitates differentiation of mouse embryonic stem cells into AHD2-expressing dopaminergic neurons. Mol Cell Neurosci 28:241–252.

Covello KL, Kehler J, Yu H, Gordan JD, Arsham AM, Hu CJ, Labosky PA, Simon MC, Keith B (2006) HIF-2α regulates Oct-4: effects of hypoxia on stem cell function, embryonic development, and tumor growth. Genes Dev 20:557–570.

Demers EJ, McPherson RJ, Juul SE (2005) Erythropoietin protects dopaminergic neurons and improves neurobehavioral outcomes in juvenile rats after neonatal hypoxia-ischemia. Pediatr Res 58:297–301.

Ema M, Hirota K, Mimura J, Abe H, Yodoi J, Sogawa K, Poellinger L, Fujii-Kuriyama Y (1999) Molecular mechanisms of transcription activation by HLF and HIF1α in response to hypoxia: their stabilization and redox signal-induced interaction with CBP/p300. EMBO J 18:1905–1914.

Ferriero DM (2005) Protecting neurons. Epilepsia 46:45–51.

Gage FH (2003) Brain, repair yourself. Sci Am 289:46–53.

Gerlach M, Gsell W, Kornhuber J, Jellinger K, Krieger V, Pantucek F, Vock R, Riederer P (1996) A post mortem study on neurochemical markers of dopaminergic, GABA-ergic and glutamatergic neurons in basal ganglia-thalamocortical circuits in Parkinson syndrome. Brain Res 741:142–152.

Greenberg DA, Jin K (2005) From angiogenesis to neuropathology. Nature 438:954–959.

Gustafsson MV, Zheng X, Pereira T, Gradin K, Jin S, Lundkvist J, Ruas JL, Poellinger L, Lendahl U, Bondesson M (2005) Hypoxia requires notch signaling to maintain the undifferentiated cell state. Dev Cell 9:617–628.

Ivanovic Z, Dello Sbarba P, Trimoreau F, Faucher JL, Praloran V (2000) Primitive human HPCs are better maintained and expanded in vitro at 1 percent oxygen than at 20 percent. Transfusion 40:1482–1488.

Iyer NV, Kotch LE, Agani F, Leung SW, Laughner E, Wenger RH, Gassmann M, Gearhart JD, Lawler AM, Yu AY, Semenza GL (1998) Cellular and developmental control of O_2 homeostasis by hypoxia-inducible factor 1 α. Genes Dev 12:149–162.

Jiang BH, Rue E, Wang GL, Roe R, Semenza GL (1996) Dimerization, DNA binding, and transactivation properties of hypoxia-inducible factor 1. J Biol Chem 271:17771–17778.

Junk AK, Mammis A, Savitz SI, Singh M, Roth S, Malhotra S, Rosenbaum PS, Cerami A, Brines M, Rosenbaum DM (2002) Erythropoietin administration protects retinal neurons from acute ischemia-reperfusion injury. Proc Natl Acad Sci USA 99:10659–10664.

Le Y, Sauer B (2000) Conditional gene knockout using cre recombinase. Methods Mol Biol 136:477–485.

Leclere N, Andreeva N, Fuchs J, Kietzmann T, Gross J (2004) Hypoxia-induced long-term increase of dopamine and tyrosine hydroxylase mRNA levels. Prague Med Rep 105:291–300.

Liss B, Haeckel O, Wildmann J, Miki T, Seino S, Roeper J (2005) K-ATP channels promote the differential degeneration of dopaminergic midbrain neurons 8:1742–1751.

Livak KJ, Schmittgen TD (2001) Analysis of relative gene expression data using real-time quantitative PCR and the 2(-Delta Delta C(T)) Method. Methods 25:402–408.

Maingay M, Romero-Ramos M, Carta M, Kirik D (2006) Ventral tegmental area dopamine neurons are resistant to human mutant alpha-synuclein overexpression. Neurobiol Dis 23:522–532.

Masliah E, Rockenstein E, Veinbergs I, Mallory M, Hashimoto M, Takeda A, Sagara Y, Sisk A, Mucke L (2000) Dopaminergic loss and inclusion body formation in alpha-synuclein mice: implications for neurodegenerative disorders. Science 287:1265–1269.

Matsuzaki H, Tamatani M, Yamaguchi A, Namikawa K, Kiyama H, Vitek MP, Mitsuda N, Tohyama M (2001) Vascular endothelial growth factor rescues hippocampal neurons from glutamate-induced toxicity: signal transduction cascades. FASEB J 15:1218–1220.

Milosevic J, Hoffarth S, Huber C, Schuler M (2003) The DNA damage-induced decrease of Bcl-2 is secondary to the activation of apoptotic effector caspases. Oncogene 22:6852–6856.

Milosevic J, Schwarz SC, Krohn K, Poppe M, Storch A, Schwarz J (2005) Low atmospheric oxygen avoids maturation, senescence and cell death of murine mesencephalic neural precursors. J Neurochem 92:718–729.

Morrison SJ, Csete M, Groves AK, Melega W, Wold B, Anderson DJ (2000) Culture in reduced levels of oxygen promotes clonogenic sympathoadrenal differentiation by isolated neural crest stem cells. J Neurosci 20:7370–7376.

Nagy A (2000) Cre recombinase: the universal reagent for genome tailoring. Genesis 26:99–109.

Orb S, Wieacker J, Labarca C, Fonck C, Lester HA, Schwarz J (2004) Knockin mice with Leu9'Ser α4-nicotinic receptors: substantia nigra dopaminergic neurons are hypersensitive to agonist and lost postnatally. Physiol Genomics 18:299–307.

Pfeifer A, Brandon EP, Kootstra N, Gage FH, Verma IM (2001) Delivery of the Cre recombinase by a self-deleting lentiviral vector: efficient gene targeting *in vivo.* Proc Natl Acad Sci USA 98:11450–11455.

Rajewsky K, Gu H, Kuhn R, Betz UA, Muller W, Roes J, Schwenk F (1996) Conditional gene targeting. J Clin Invest 98:600–603.

Ryan HE, Lo J, Johnson RS (1998) HIF-1α is required for solid tumor formation and embryonic vascularization. EMBO J 17:3005–3015.

Ryan HE, Poloni M, McNulty W, Elson D, Gassmann M, Arbeit JM, Johnson RS (2000) Hypoxia-inducible factor-1α is a positive factor in solid tumor growth. Cancer Res 60:4010–4015.

Sakanaka M, Wen TC, Matsuda S, Masuda S, Morishita E, Nagao M, Sasaki R (1998) In vivo evidence that erythropoietin protects neurons from ischemic damage. Proc Natl Acad Sci USA 95:4635–4640.

Schnell PO, Ignacak ML, Bauer AL, Striet JB, Paulding WR, Czyzyk-Krzeska MF (2003) Regulation of tyrosine hydroxylase promoter activity by the von Hippel-Lindau tumor suppressor protein and hypoxia-inducible transcription factors. J Neurochem 85:483–491.

Semenza GL (1999) Regulation of mammalian O_2 homeostasis by hypoxia-inducible factor 1. Annu Rev Cell Dev Biol 15:551–578.

Sharpless NE, DePinho RA (2004) Telomeres, stem cells, senescence, and cancer. J Clin Invest 113:160–168.

Silver I, Erecinska M (1998) Oxygen and ion concentrations in normoxic and hypoxic brain cells. Adv Exp Med Biol 454:7–16.

Soucek T, Cumming R, Dargusch R, Maher P, Schubert D (2003) The regulation of glucose metabolism by HIF-1 mediates a neuroprotective response to amyloid beta peptide. Neuron 39:43–56.

Storch A, Paul G, Csete M, Boehm BO, Carvey PM, Kupsch A, Schwarz J (2001) Long-term proliferation and dopaminergic differentiation of human mesencephalic neural precursor cells. Exp Neurol 170:317–325.

Studer L, Csete M, Lee SH, Kabbani N, Walikonis J, Wold B, McKay R (2000) Enhanced proliferation, survival, and dopaminergic differentiation of CNS precursors in lowered oxygen. J Neurosci 20:7377–7383.

Sun Y, Jin K, Xie L, Childs J, Mao XO, Logvinova A, Greenberg DA (2003) VEGF-induced neuroprotection, neurogenesis, and angiogenesis after focal cerebral ischemia. J Clin Invest 111:1843–1851.

Tomita S, Ueno M, Sakamoto M, Kitahama Y, Ueki M, Maekawa N, Sakamoto H, Gassmann M, Kageyama R, Ueda N, Gonzalez FJ, Takahama Y (2003) Defective brain development in mice lacking the Hif-1α gene in neural cells. Mol Cell Biol 23:6739–6749.

Wenger RH (2002) Cellular adaptation to hypoxia: O_2-sensing protein hydroxylases, hypoxia-inducible transcription factors, and O_2-regulated gene expression. FASEB J 16:1151–1162.

Yasuhara T, Shingo T, Muraoka K, Kameda M, Agari T, Wen Ji Y, Hayase H, Hamada H, Borlongan CV, Date I (2005) Neurorescue effects of VEGF on a rat model of Parkinson's disease. Brain Res 1053:10–18.